

High-accuracy Hamiltonian learning via delocalized quantum state evolutions

Davide Rattacaso¹, Gianluca Passarelli², and Procolo Lucignano¹

¹Dipartimento di Fisica “E. Pancini”, Università di Napoli Federico II, Complesso di Monte Sant’Angelo, via Cinthia, Napoli 80126, Italy

²CNR-SPIN, c/o Complesso di Monte Sant’Angelo, via Cinthia, Napoli 80126, Italy

Learning the unknown Hamiltonian governing the dynamics of a quantum many-body system is a challenging task. In this manuscript, we propose a possible strategy based on repeated measurements on a single time-dependent state. We prove that the accuracy of the learning process is maximized for states that are delocalized in the Hamiltonian eigenbasis. This implies that delocalization is a quantum resource for Hamiltonian learning, that can be exploited to select optimal initial states for learning algorithms. We investigate the error scaling of our reconstruction with respect to the number of measurements, and we provide examples of our learning algorithm on simulated quantum systems.

1 Introduction

Thanks to the enormous progress in manufacturing and controlling quantum devices made out of an increasingly large number of qubits, we are now entering the era of Noisy Intermediate-Scale Quantum technology [1]. Relevant progresses have been made in controlling quantum degrees of freedom on different platforms [2–4]. However, to some extent the true Hamiltonian, governing the dynamics of these systems is often (at least) partially unknown. In this context, the major challenge is then to infer a realistic Hamiltonian model of the quantum system that can match the experimental data, guided by physical intuition. By querying the device (assumed a black box), one can measure the time evolution of several observables in order to learn the system Hamiltonian. This process, known as Hamiltonian learning, has been fundamental over the years for the

Davide Rattacaso: davide.rattacaso@unina.it

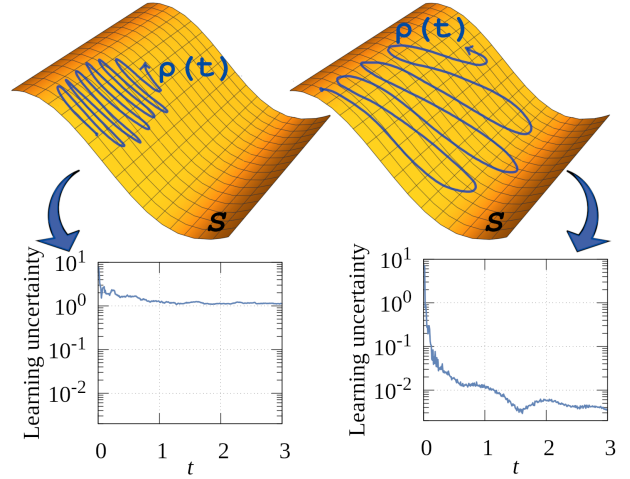


Figure 1: The larger is the capability of the state $\rho(t)$ to explore the space of states S , the larger is the amount of information obtained through the learning process, and, consequently, the smaller is the uncertainty in reconstructing the Hamiltonian.

validation of theoretical models, where the observation of the system evolution aims to characterize the unknown parameters of the model and establish its plausibility, and is now centralizing the attention of the scientific community due to its relevance for quantum technologies and quantum computation [5–28]. Applications of Hamiltonian learning range from the verification of the performances of quantum devices [29–33], to quantum error correction [34], to the design, characterization and calibration of quantum devices [26, 27, 34].

The performance of a Hamiltonian learning algorithm is determined by the scaling of the relative uncertainty of the reconstructed Hamiltonian as a function of the computational effort required, which, in many relevant situations, is given by the number N_S of experiments, or shots. Each shot begins with a state preparation and ends with a measurement in the computational basis. To fully

reconstruct a quantum Hamiltonian, its action on a basis of the Hilbert space must be known. As a result, a number of initial states that is exponential in the systems size is needed for a full process tomography, leading to an exponential overhead in the number of shots required for learning.

When the Hamiltonian is the span of local interactions, it has been proven that a polynomial number of experiments is sufficient to fully reconstruct its couplings [35]. Significant examples in this direction are the reconstruction of the system Hamiltonian from short-time evolutions [25] and taking advantage from the exploitation of symmetries of the unknown Hamiltonian [26]. In these works, locality is a resource for the learning process.

In this paper, we focus on properties of the state (rather than the Hamiltonian) and we propose a novel algorithm that requires measurements of a single time-dependent quantum state. The main idea is to take benefit of quantum superposition. As depicted in Figure 1, indeed, some states are able to explore a significant portion of the space of states S during their time evolution and therefore encode enough information to completely reconstruct the Hamiltonian generating their dynamics. Using analytical arguments and numerical examples, we show that the accuracy of the method proposed is related to the delocalization of the initial state in the Hamiltonian eigenstates. To this aim, we prove an analytical relationship between the inverse participation ratio (IPR) [36–38] of the initial state, and the information matrix that measures the amount of information acquired in the learning process. Equally weighted superpositions of the Hamiltonian eigenstates explore a large sample of the space of states and provide the maximum amount of information about the system Hamiltonian. In other words, delocalization is a resource for Hamiltonian learning. This opens a new perspective on the application of quantum information theory to the study of out-of-equilibrium quantum systems [36, 39]. As a proof of concepts, we apply our method to learn the Hamiltonian of systems of few superconducting qubits, highlighting its relevance to gate-based quantum computation. In this setting, we exploit state tomography to define a simple algorithm that clarifies the relationship between delocalization and learning. Full state tomography requires an exponential amount of resources in

the system size. However, scaling to large system sizes is out of the purposes of this manuscript.

2 Hamiltonian learning algorithm

To fully represent the information content of the system state, we define a basis $\mathcal{B} = \{O_\alpha\}$ for the space of Hermitian operators, orthonormal with respect to the Hilbert-Schmidt product $(A, B) = \text{Tr}(AB)$. In this basis, the system density matrix $\rho(t)$ can be expanded as $\rho(t) = \sum_\alpha r_\alpha(t)O_\alpha$ where $r_\alpha(t) \equiv \text{Tr}(O_\alpha\rho(t))$ are the components of $\rho(t)$ over \mathcal{B} and are the expectation values of the observables O_α over the state $\rho(t)$. If we measured the coefficients $r_\alpha(t_n)$ at a collection of N_T times $\{t_n\} \equiv \{0, \delta t, \dots, (N_T - 1)\delta t\}$, we would have a time-dependent state tomography. Repeating each measurement N_M times, the uncertainty on each observables is $\sigma(r_\alpha(t_n)) = \sqrt{\text{Tr}(O_\alpha^2\rho(t_n))/N_M}$. In superconducting quantum processing units, measurements are always performed in the computational basis, i. e., in the basis of simultaneous eigenstates of the single-qubit operators σ_i^z . Measuring observables that do not commute with σ_i^z , such as $\sigma_i^{x,y}$, can be done by first rotating the system state so that $\sigma_i^{x,y} \rightarrow \sigma_i^z$. This means that we need to perform 3 measurements per qubit in order to have full information about the system state. As a consequence, in a system of N_q qubits the number experiment shots needed for a full state tomography is $N_S = 3^{N_q} N_T N_M$.

In general, the unknown Hamiltonian is a Hermitian operator that can be expanded in the (exponentially large in the system size) basis \mathcal{B} . However, realistic Hamiltonians often have symmetries and/or locality constraints that can be identified resorting to first-principle theoretical models [40]. Hence, we can write the unknown Hamiltonian as the span of a set of local Hermitian and traceless operators $\mathcal{B}_L = \{L_i\}$ that represent the relevant interactions between the constituents of the system: $H = \sum_i h_i L_i$. Remarkably, the locality constraint implies that the number of L_i in \mathcal{B}_L is at most polynomial in the system size [28].

We want to exploit the information extracted from the state evolution via a full tomography to learn the couplings h_i of the system Hamiltonian H . Assuming that the system evolves unitarily according to the Liouville-von Neumann equation

$\dot{\rho} = -i[H, \rho]$ (here and in the following $\hbar = 1$), the system state at a time t_{n+1} is related to $\rho(t_n)$ via the equation

$$\frac{\rho(t_{n+1}) - \rho(t_n)}{\delta t} + i \sum_i h_i [L_i, \rho(t_n)] = R_n \delta t, \quad (1)$$

where $R_n = \frac{-[H, [H, \rho(t_n)]]}{2}$ is the remainder of the Taylor expansion at the first order of $\rho(t_{n+1})$, for $t^* \in [t_n, t_{n+1}]$.

In an ideal experiment, δt could be made arbitrarily small and the uncertainty on the states $\rho(t_n)$ would vanish as well. As a consequence, the optimal couplings $h_i^{(\text{opt})}$ are the ones that minimize the Frobenius norm of the LHS of Eq. (1) at each time, that is:

$$f(\vec{h}) = C - 2 \sum_i h_i B_i + \sum_{ij} V_{ij} h_i h_j, \quad (2)$$

where

$$V_{ij} = - \sum_n \text{Tr}([L_i, \rho(t_n)][L_j, \rho(t_n)]) , \quad (3)$$

$B_j = \sum_n \text{Tr}(-i[L_j, \rho(t_n)](\rho(t_{n+1}) - \rho(t_n))/\delta t)$, and $C = \sum_n \text{Tr}((\rho(t_{n+1}) - \rho(t_n))^2/\delta t^2)$. We call the matrix V_{ij} the Total Quantum Covariance Matrix (TQCM).

The optimal couplings are such that the gradient of $f(\vec{h})$ is null. When the TQCM is invertible these couplings can be written as

$$h_i^{(\text{opt})} = \sum_j (V^{-1})_{ij} B_j, \quad (4)$$

Eq. (4) can serve to our goal if the kernel of V_{ij} is empty, otherwise, the experimental data are insufficient to specify the system Hamiltonian, meaning that different Hamiltonians can produce the same observables.

3 Uncertainty estimation

In real experiments, the expectation values $r_\alpha(t_n)$ are affected by statistical uncertainties. Moreover, the time interval δt between measurements cannot be reduced to zero, and the remainder R_n has to be considered as a systematic source of error for the estimated derivatives $(\rho(t_{n+1}) - \rho(t_n))/\delta t$. These contributions determine a total uncertainty δB_i on the vector B_i . As a consequence, the Hamiltonian couplings are

known up to an uncertainty δh_i and any Hamiltonian $H = \sum_i h_i L_i$ with $|h_i - h_i^{(\text{opt})}| < \delta h_i$ is compatible with the dynamics observed through the measurement of the local expectation values $r_\alpha(t_n)$. Remarkably, since we perform tomography even at the initial time, state preparation errors do not directly affect the uncertainty on the reconstructed Hamiltonian.

As we show in Appendix A, both the statistical and the systematic part of the uncertainty δB_i can be upper-bounded by a function that does not depend on the specific evolution of the system, but only on the Hamiltonian norm, the total number of repetitions N_M , time steps N_T and the number of qubits N_q . Relating the uncertainty δB_i to the uncertainty δh_i through Eq. (4) and considering the relationship between the vector norm of the exact couplings $\|\vec{h}\|$ and the operator norm $\|H\|_{\text{op}}$, we can extend this bound to the relative error

$$\varepsilon \equiv \|\vec{h}^{(\text{opt})} - \vec{h}\|/\|\vec{h}\| \quad (5)$$

on the reconstructed Hamiltonian:

$$\varepsilon \leq \sqrt{l \text{Tr} \left[\left(\frac{V_{ij}}{\|L\|_{\text{op}}^2 N_T} \right)^{-2} \right]} \times \left(16 \frac{(3/2)^{N_q}}{\sqrt{N_S}} + 4\|H\|_{\text{op}} \delta t \right), \quad (6)$$

where l is the number of couplings of the Hamiltonian and, without loss of generality, we suppose that $\|L_i\|_{\text{op}} = \|L\|_{\text{op}} \forall i$. Remarkably, this reconstruction error is not affected by the derivative uncertainty, inversely proportional to the time step, which decreases the accuracy of the learning protocols based on short-time evolution[25]. This feature can represent a significant advantage in characterizing devices with a high temporal resolution.

In Eq. (6), the upperbound on the relative error only depends on the system evolution through the eigenvalues of the TQCM. In particular, the larger are these eigenvalues, the larger is the amount of information about the system Hamiltonian that we gain by observing the state evolution. Conversely, when some eigenvalue of the TQCM goes to zero and the matrix is not invertible, the uncertainty diverges, signaling that the information acquired during the experiment is not sufficient for Hamiltonian learning. We can clearly

see the statistical meaning of the TQCM: Eq. (6) is analogous to a Cramer-Rao bound on the error on the estimated Hamiltonian [27, 41], where the TQCM takes the role of an information matrix. While the spectrum of V_{ij} estimates the total amount of information about the Hamiltonian that we have gained by observing the state during its evolution, at any fixed time t_n , the spectrum of

$$V_{ij,n} \equiv -\text{Tr}([L_i, \rho(t_n)][L_j, \rho(t_n)]) \quad (7)$$

estimates the amount of information about the Hamiltonian gained by observing the short-time evolution around t_n . Both V_{ij} and $V_{ij,n}$ depend on the initial state preparation and on the consequent evolution. The quantum state preparation of the initial state is crucial to the success of the algorithm, optimal initial states are those maximizing the amount of information gained by observing the evolution, hence, minimizing the uncertainty on the reconstructed Hamiltonian.

4 Information and inverse participation ratio

Schrodinger's evolution often delocalizes states in the Hilbert space. In this section, we show that the more the state samples the Hilbert space, the more information we gain about the system Hamiltonian.

As shown in Eq. (6), the largest contribution to the relative error comes from the minimum eigenvalue of the TQCM. The TQCM is the sum over the different time steps of the covariance matrices $V_{ij,n}$. Following the definition of Eq. (7), these are positive semi-definite. Evolution of highly delocalized states generates very different covariance matrices at different times. In this case, we speculate that the eigenvalues of the TQCM exponentially increase for an initial transient, corresponding to the time spent by the state $\rho(t)$ in exploring the space of states before returning close to its previous orbit. The larger is the sample of the space of states explored by $\rho(t)$ during its evolution, the larger will be the amount of information on the system Hamiltonian gained by observing the evolution of $\rho(t)$.

Quantitatively, we show that a good estimation of the information obtained in the learning process is the IPR of the initial state in the Hamiltonian eigenstates [36–38]. If the system Hamiltonian is $H = \sum_{\alpha} E_{\alpha} |\alpha\rangle\langle\alpha|$ and the initial state

of the system is $|\psi\rangle = \sum_{\alpha} a_{\alpha} |\alpha\rangle$, the IPR is defined as $\text{IPR}(\psi, H) = \sum_{\alpha} |a_{\alpha}|^4$. Therefore, the IPR measures the spreading of the initial state in the Hamiltonian eigenstates: the lower is the IPR, the more the initial state spreads out. This is also an estimation of the capability of the state of sampling the Hilbert space uniformly during the evolution, in analogy with the ergodic hypothesis. Indeed, the time average of an observable A during the evolution is $\bar{A} = \text{Tr}(\bar{\rho}A)$, where $\bar{\rho} = \sum |a_{\alpha}|^2 |\alpha\rangle\langle\alpha|$ is the dephased state. As a consequence, when the IPR is minimum ($\text{IPR}_{\min} = 1/2^{N_q}$) all the populations of $\bar{\rho}$ are equal and the time average becomes an average on the energy eigenstates with equal weights.

The relationship between the uncertainty on the reconstructed Hamiltonian and the IPR will be clear in the numerics that follow. However, a simple general argument is given here, showing that the states with a small IPR are associated with large eigenvalues of the TQCM and, due to Eq. (6), with a small error of the reconstructed Hamiltonian.

Please note that in order to calculate the IPR, one needs to know the Hamiltonian eigenstates $|\alpha\rangle$. This may sound odd, as the Hamiltonian itself is unknown in general. However, in our examples we apply our method to learn “known” Hamiltonians, and we can explicitly calculate the IPR. In possible practical applications, this is not the case, but one could resort to adaptive learning approaches as in Ref. [27]. Starting from a state minimizing the IPR over the eigenstates of a guessed Hamiltonian, one can iteratively obtain better estimates of the target Hamiltonian.

We consider $\rho(t)$ as a pure state $\rho(t) = |\psi(t)\rangle\langle\psi(t)|$, where $|\psi(0)\rangle = \sum_{\alpha} a_{\alpha} |\alpha\rangle$ and $|\alpha\rangle$ are the eigenstates of the unknown system Hamiltonian. The eigenvalues ω_i of the TQCM can be written as $\omega_i = \sum_{jj'} V_{jj'} a_j^{(i)} a_{j'}^{(i)}$, in terms of the corresponding normalized eigenvectors $a_j^{(i)}$. Defining the local operators $A_i \equiv \sum_j a_j^{(i)} L_j$, the eigenvalues ω_i of the TQCM of Eq. (3) read:

$$\begin{aligned} \omega_i &= -\sum_n^{N_T} \text{Tr}([A_i, \rho(t_n)][A_i, \rho(t_n)]) \\ &= 2 \sum_n^{N_T} \left(\langle\psi(t_n)|A_i^2|\psi(t_n)\rangle - \langle\psi(t_n)|A_i|\psi(t_n)\rangle^2 \right). \end{aligned}$$

If the time-step δt is sufficiently small, this sum can be approximated by an integral: Considering

that $|\psi(t)\rangle = \sum_{\alpha} a_{\alpha} |\alpha\rangle e^{-iE_{\alpha}t}$, for $\delta t \rightarrow 0$ these eigenvalues can be written as integrals of local correlations:

$$\begin{aligned} \omega_i &\approx \frac{2N_T}{T} \int_0^T dt \left(\langle \psi(t) | A_i^2 | \psi_n \rangle - \langle \psi(t) | A_i | \psi(t) \rangle^2 \right) \\ &= \frac{2N_T}{T} \int_0^T dt \left(\sum_{\alpha\beta} a_{\alpha} a_{\beta}^* \langle \alpha | A_i^2 | \beta \rangle e^{-it(E_{\alpha} - E_{\beta})} \right. \\ &\quad \left. - \sum_{\alpha\beta\gamma\delta} a_{\alpha} a_{\beta}^* a_{\gamma} a_{\delta}^* \langle \alpha | A_i | \beta \rangle \langle \gamma | A_j | \delta \rangle \right) \\ &\quad \times e^{-it(E_{\alpha} - E_{\beta} + E_{\gamma} - E_{\delta})}. \end{aligned} \quad (8)$$

At this point we impose a non-degeneracy and non-resonance condition on the system Hamiltonian H . The non-resonance condition consists in the fact that $E_{\alpha} - E_{\beta} + E_{\gamma} - E_{\delta} = 0$ if and only if $E_{\alpha} = E_{\beta}$ and $E_{\gamma} = E_{\delta}$ or $E_{\beta} = E_{\gamma}$ and $E_{\alpha} = E_{\delta}$. This condition is automatically satisfied by any Hamiltonian that is not fine-tuned, so we can assume its validity for the real unknown Hamiltonian. In this way, after a time transient T_e that is the equilibration time of the system [36], the oscillating terms vanish and the previous equation becomes

$$\begin{aligned} \omega_i &\approx 2N_T \left[\sum_{\alpha} |a_{\alpha}|^2 \langle \alpha | A_i^2 | \alpha \rangle \right. \\ &\quad \left. - \sum_{\alpha\beta} |a_{\alpha}|^2 |a_{\beta}|^2 \left(\langle \alpha | A_i | \alpha \rangle \langle \beta | A_i | \beta \rangle + |\langle \alpha | A_i | \beta \rangle|^2 \right) \right]. \end{aligned} \quad (9)$$

or, equivalently,

$$\omega_i \approx 2N_T [\text{Tr}(\bar{\rho} A_i^2) - (\text{Tr}^2(\bar{\rho} A_i) + \text{Tr}(\bar{\rho}^2 A_i^2))]. \quad (10)$$

After the equilibration time these eigenvalues become linear in the number of time steps, with a coefficient $[\text{Tr}(\bar{\rho} A_i^2) - (\text{Tr}^2(\bar{\rho} A_i) + \text{Tr}(\bar{\rho}^2 A_i^2))]$ that corresponds to a measure of variance for A_i in the dephased state $\bar{\rho}$. The positive contribution to this variance comes from the term $\text{Tr}(\bar{\rho} A_i^2)$, while the negative contributions come from $\text{Tr}^2(\bar{\rho} A_i)$ and $\text{Tr}(\bar{\rho}^2 A_i^2)$. When the IPR of the system state is near to its minimum, the dephased state is well approximated by the totally mixed state and, since the L_i 's are traceless, the term $\text{Tr}^2(\bar{\rho} A_i)$ vanishes. The remaining negative contribution also decreases in magnitude with the IPR, that can be written as $\text{Tr}(\bar{\rho}^2)$. We can conclude that minimizing the IPR is a good strategy to generate larger eigenvalues ω_i of the TQCM.

The optimal initial states, minimizing the IPR and therefore optimizing the learning process, are thus

$$|\psi_{\text{opt}}\rangle = \sqrt{2^{-N_q}} \sum_{\alpha} e^{i\phi_{\alpha}} |\alpha\rangle \quad (11)$$

where the ϕ_{α} 's are arbitrary phases that we can fix to zero.

Due to the beneficial effect of delocalization, one could wonder if mixed states can also be considered a resource for learning algorithms. However, since the TQCM in Eq. (3) is related to the trace of ρ^2 , we expect states with smaller purity to have a smaller TQCM and to determine a worse accuracy.

5 Simulations

We have applied our Hamiltonian learning method to some few-qubit problems, in order to verify our predictions about the error scaling in Eq. (6) and the relationship between the TQCM and the IPR in Eq. (10). After focusing on a simple two-qubit problem, we discuss a three-qubit model with random couplings and we use Qiskit [42] to show how to apply our method to a real quantum processor.

In order to apply our learning procedure, we first choose a Hamiltonian H and generate the evolution of the expectation values of the basis elements $\{O_{\alpha}\}$ by numerically integrating the Liouville equation for a set of initial states, corresponding to different initial configurations for the experiment with different IPRs. The effect of the statistical error is simulated by adding a uniform random noise with amplitude $1/\sqrt{2^{N_q} N_M}$ to each expectation value. Then, given the simulated expectation values $r_{\alpha}(t_n)$, we apply our method to find the optimal Hamiltonian $H^{(\text{opt})} = \sum_i h_i^{(\text{opt})} L_i$. The success of the learning procedure can be checked comparing H with $H^{(\text{opt})}$. In particular we analyze the relative error ε and the TQCM for each initial state and for different numbers of time steps N_T , corresponding to different total observation times. We also estimate the relationship between the IPR and the information gained in the experiment, measured by the eigenvalues of the TQCM. Finally, we also calculate the optimal initial state $|\psi_{\text{opt}}\rangle$ for each Hamiltonian and exploit it for an optimal learning.

5.1 Cross-resonance gate

We focus on a quantum system representing a two-qubit device governed by the typical Hamiltonian of a cross-resonance gate [40, 43–45]. The implementation of this gate, consisting in two transmon qubits coupled by a bus resonator, is fundamental to realize the CNOT gate for universal quantum computation. The Hamiltonian that we want to reconstruct is

$$H = -1.548 \mathbb{1} \otimes \sigma_x - 0.004 \mathbb{1} \otimes \sigma_y + 0.006 \mathbb{1} \otimes \sigma_z + 9.578 \sigma_z \otimes \mathbb{1} + 5.316 \sigma_z \otimes \sigma_x - 0.225 \sigma_z \otimes \sigma_y - 0.340 \sigma_z \otimes \sigma_z, \quad (12)$$

where the couplings are taken from Ref. [46] and the energies are expressed in MHz. The optimal Hamiltonian is then found as the span of the operators $\{L_i\} = \{\mathbb{1} \otimes \sigma_x, \mathbb{1} \otimes \sigma_y, \mathbb{1} \otimes \sigma_z, \sigma_z \otimes \mathbb{1}, \sigma_z \otimes \sigma_x, \sigma_z \otimes \sigma_y, \sigma_z \otimes \sigma_z\}$. This choice is justified by first-principles studies [45].

The Hamiltonian learning algorithm is performed with a time step $\delta t = 0.01$, $N_M = 1000$ measurement repetitions and a total number of shots $N_S = 3 \times 10^6$, for four initial states with different IPR. The reconstructed Hamiltonian couplings for each initial state (with its IPR) are shown in Table 1. We observe that when the initial state has a small IPR, the accuracy is maximized.

In Fig. 2(a) we show the behavior of the relative reconstruction error as a function of the number of experiment shots N_S . N_S is increased by increasing the number of time steps N_T and, consequently, the observation time. Different curves represent states with different IPR. The numerical simulations confirm our predictions: after a

Table 1: Estimated Hamiltonian coupling for different initial states with the corresponding IPR in parentheses, with $\delta t = 0.01$, $N_M = 1000$ and $N_S = 3 \times 10^6$. We define $|\rightarrow\rightarrow\rangle \equiv (|\uparrow\rangle + |\downarrow\rangle) \otimes (|\uparrow\rangle + |\downarrow\rangle)/2$ and $|\psi_{\text{Bell}}^+\rangle \equiv (|\uparrow\uparrow\rangle + |\downarrow\downarrow\rangle)/\sqrt{2}$.

Term	Target	$ \uparrow\uparrow\rangle$ (0.503)	$ \rightarrow\rightarrow\rangle$ (0.498)	$ \psi_{\text{Bell}}^+\rangle$ (0.251)	$ \psi_{\text{opt}}\rangle$ (0.25)
$\mathbb{1} \otimes \sigma_x$	-1.548	2.142	-1.143	-1.543	-1.542
$\mathbb{1} \otimes \sigma_y$	-0.004	1.021	-0.024	-0.011	0.000
$\mathbb{1} \otimes \sigma_z$	0.006	1.073	-0.017	-0.009	0.023
$\sigma_z \otimes \mathbb{1}$	9.578	-1.418	9.748	9.556	9.553
$\sigma_z \otimes \sigma_x$	5.316	1.627	5.089	5.301	5.295
$\sigma_z \otimes \sigma_y$	-0.225	-1.254	-0.218	-0.216	-0.237
$\sigma_z \otimes \sigma_z$	-0.340	-1.409	-0.328	-0.324	-0.357

transient in which the error decreases exponentially in the number of time steps, the final error converges to values that are smaller for states with a smaller IPR. Optimal results are obtained when the initial state is $|\psi_{\text{opt}}\rangle$. In Fig. 2(b), we show the behavior of the Frobenius norm of the inverse TQCM times the number of time steps, as a function of the experiment shots. We observe a correlation between the exponential decrease of the reconstruction error and the exponential decrease of this quantity, which saturates to a value proportional to the IPR. This is consistent with our theoretical predictions.

The relationship between IPR and information is shown in Fig. 2(c), where, for a set of random initial states, we represent the IPR and the Frobenius norm of the inverse TQCM at the final time. We observe that these functions are positively correlated for small values of the TQCM, confirming the predictions of Eq. (10): to improve the performance of the learning algorithm, we have to prepare initial states with a small IPR. In particular, the best possible performance corresponds to the minimum IPR, which, for a 2-qubit system, is $\text{IPR}_{\text{min}} = 1/4$.

5.2 Random 2-body Hamiltonian

Here we test the learning algorithm on a system evolving with a random Hamiltonian

$$H = \sum_i h_i L_i, \quad (13)$$

where $h_i \in [-5, 5]$ and the L_i are all the two-spins interactions acting on a three-spins system, represented by tensor products of two Pauli operators and the identity operator. The Hamiltonian learning algorithm is performed with a time step $\delta t = 0.01$, $N_M = 1000$ measurement repetitions and a maximum number of 370 time steps.

The relative error of the reconstruction and the behaviour of the TQCM are shown in Figure 3 Panels (a) and (b). In Figure 3 Panel (c) we show the IPR and the Frobenius norm of the inverse TQCM for a collection of random states at large final time. The validity of theoretical predictions about the optimality of low IPR states is particularly evident in Panels (b) and (c), where the statistical and systematic contributions to uncertainty are not considered.

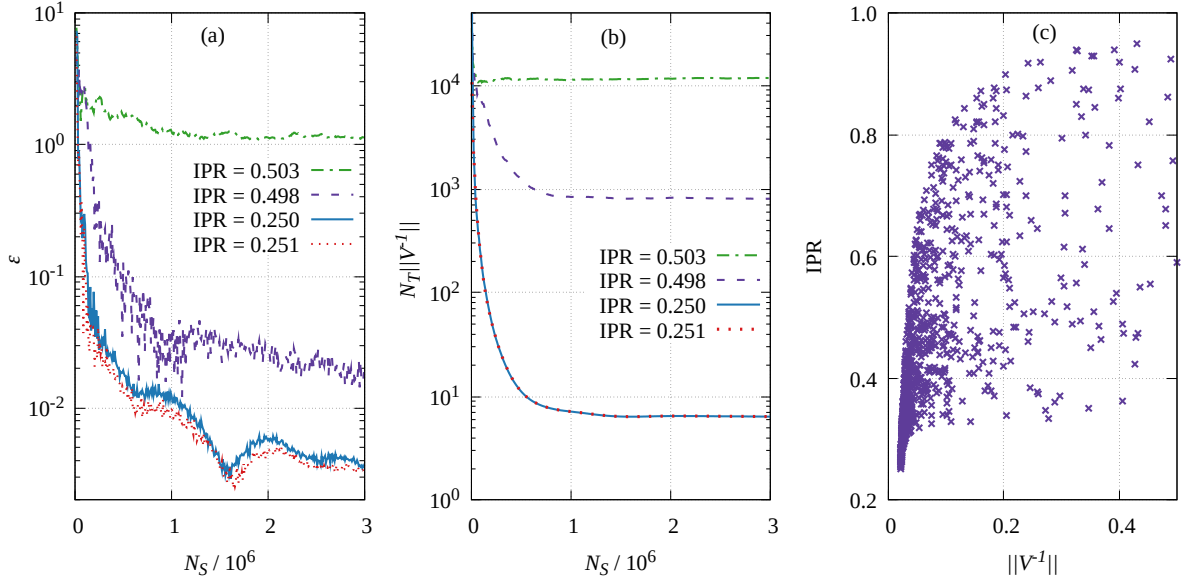


Figure 2: (a) relative reconstruction error and (b) Frobenius norm of the inverse TQCM multiplied by N_T , as a function of N_S for the cross-resonance gate Hamiltonian in Eq. (12), with $\delta t = 0.01$, $N_M = 1000$ and $N_S = 9 \times N_M \times N_S$, for different initial states with different IPR. (c) IPR and Frobenius norm of the inverse TQCM for a collection of random states at large final time for the cross-resonance gate Hamiltonian, with $N_T = 300$.

5.3 IBM Q FakeAthens processor

We test the learning algorithm on a simulated quantum processor, the FakeAthens processor, using Qiskit [42]. Our approach, from state preparation to the final measurements, can be identically extended to any quantum processor. The present simulator considers a two qubits system and take into account errors in state preparation and in measurements. We remark that, due to preparation errors, the starting state is not a pure state, nevertheless our method is applicable.

We execute a time-dependent unitary gate, represented in the computational basis as

$$U(t) = \begin{pmatrix} \cos(4\pi t) & -i \sin(4\pi t) & 0 & 0 \\ -i \sin(4\pi t) & \cos(4\pi t) & 0 & 0 \\ 0 & 0 & 1 & 0 \\ 0 & 0 & 0 & 1 \end{pmatrix}. \quad (14)$$

We know that this gate is obtained through the cross-resonance mechanism illustrated in our first example, hence we look at a parent Hamiltonian that is spanned by the same operators:

$$\{L_i\} = \{\mathbb{1} \otimes \sigma_x, \mathbb{1} \otimes \sigma_y, \mathbb{1} \otimes \sigma_x, \sigma_z \otimes \mathbb{1}, \sigma_z \otimes \sigma_x, \sigma_z \otimes \sigma_y, \sigma_z \otimes \sigma_z\}. \quad (15)$$

Since in this case we do not know *a priori* the real system Hamiltonian, in Figure 4 Panels (a)

and (b) we show, for increasing total observation time corresponding to an increasing number of shots, the Hamiltonian couplings learned with different initial states, respectively the states $|\downarrow\downarrow\rangle$ and the Bell state $(|\uparrow\uparrow\rangle + |\downarrow\downarrow\rangle)/\sqrt{2}$. Looking at Panel 4(c) we can see that a smaller uncertainty, and therefore a more reliable Hamiltonian reconstruction is obtained when the starting state is the Bell state, with smaller IPR [Panel (b)].

6 Conclusions and outlook

We have introduced a Hamiltonian learning algorithm whose global accuracy depends on the IPR of the starting state in the Hamiltonian eigenstates. The reconstruction error decays exponentially at short times and equilibrate to a value proportional to the IPR. Our results establish a direct connection between state delocalization and Hamiltonian learning. We conclude that delocalization can be exploited to drastically improve the efficiency of Hamiltonian learning algorithms. Moreover, since the TQCM can be interpreted as an information matrix on the space of states, the relationship between the time evolution of the QCM and the IPR of the state opens a new perspective on the information-geometric approach to the investigation of many-body quantum sys-

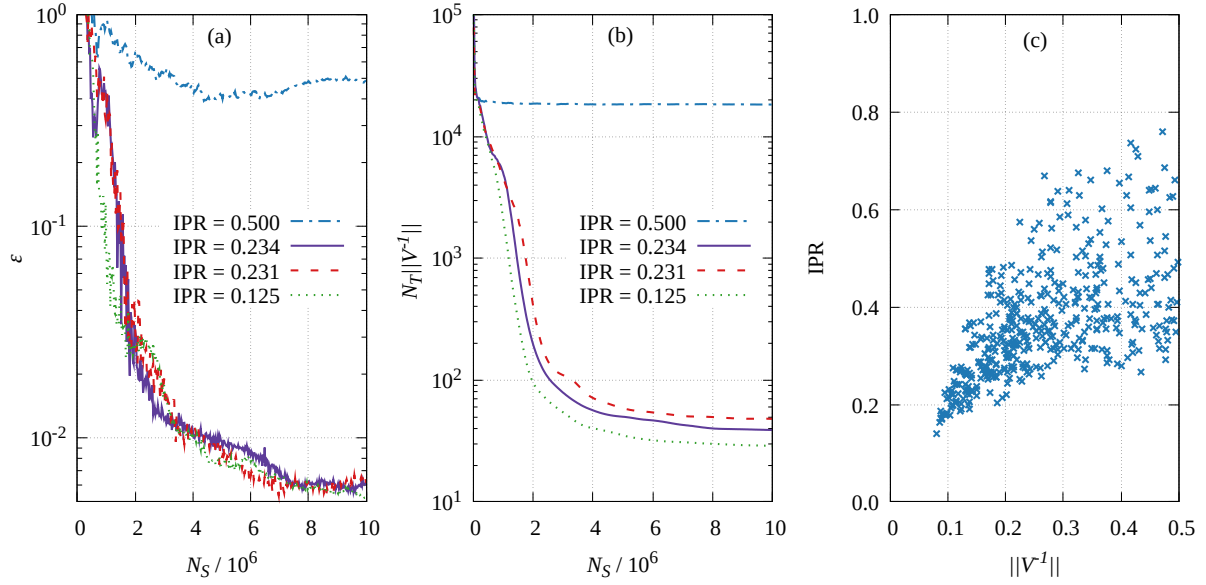


Figure 3: (a) relative reconstruction error and (b) Frobenius norm of the inverse TQCM multiplied by N_T , as a function of N_S , with $\delta t = 0.01$, $N_M = 1000$ and $N_S = 27 \times N_M \times N_S$. The initial states are: an equal weighted superposition of two Hamiltonian eigenstates with IPR = 0.5, the GHZ state with IPR ≈ 0.231 , $|\uparrow\uparrow\uparrow\rangle$ with IPR ≈ 0.234 , and $|\psi_{\text{opt}}\rangle$ with IPR = 0.125. (c) IPR and Frobenius norm of the inverse TQCM for a collection of random states at large final time, $N_T = 370$.

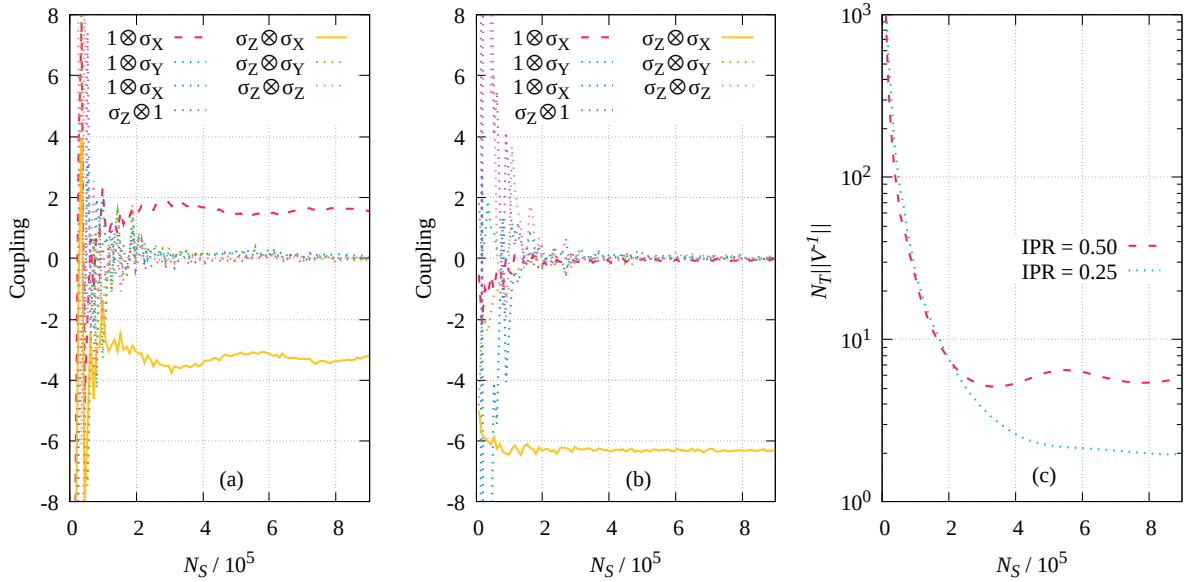


Figure 4: Panels (a) and (b): reconstructed Hamiltonian couplings at increasing number of shots, corresponding to longer observation time, for $N_M = 1000$, $\delta t = 0.01$ and maximum number of time steps $N_{T,\text{max}} = 100$. Panel (a): initial state $|\downarrow\downarrow\rangle$, Panel (b): initial state is the Bell state. Panel (c): Frobenius norm of the inverse TQCM multiplied by N_T , as a function of N_S for the two initial states.

tems [47–50]: the equilibration and ergodicity of a closed quantum system [39] can reflect on its out-of-equilibrium geometry [51].

Remarkably, our method is designed to reconstruct the system Hamiltonian from a generic quantum state, either pure or mixed. This feature is appealing for the application to real devices, where the preparation of the initial state can be affected by SPAM noise. In this regard, a natural extension of the methods described in this paper is the design of Lindbladian learning algorithms to deal with open quantum systems.

After the initial time transient, the errors on the learning is negligible and our results show an excellent agreement between the true Hamiltonian used to generate the dynamics and our optimal reconstructed Hamiltonian. The price to pay is to perform a complete tomography of the state at different times, obtained by measuring all the observables in $\{O_\alpha\}$. The number of these observables increases exponentially in the system size, rendering our approach too demanding for large systems. This great effort in collecting expectation values is partially rewarded by an exponentially decreasing relative error [Eq. (6)]. In perspective, we could perform a partial tomography and only measure the expectation values of the polynomial set of observables that optimizes the accuracy. These observables, as well as optimal initial states, could be selected through adaptive learning strategies, in analogy with Ref. [27], where the role of the TQCM is taken by the Fisher Information Matrix.

We thank G. Acanfora, A. Dutt, R. Fazio, A. Mezzacapo, and A. Russomanno for useful discussions and support. This work has been funded by project code PIR01_00011 “IBiSCo”, PON 2014-2020, for all three entities (INFN, UNINA and CNR).

References

- [1] John Preskill. Quantum computing in the nisq era and beyond. *Quantum*, 2:79, Aug 2018. ISSN 2521-327X. DOI: [10.22331/q-2018-08-06-79](https://doi.org/10.22331/q-2018-08-06-79). URL <http://dx.doi.org/10.22331/q-2018-08-06-79>.
- [2] Sepehr Ebadi, Tout T. Wang, Harry Levine, Alexander Keesling, Giulia Semeghini, Ahmed Omran, Dolev Bluvstein, Rhine Samajdar, Hannes Pichler, Wen Wei Ho, Soonwon Choi, Subir Sachdev, Markus Greiner, Vladan Vuletić, and Mikhail D. Lukin. Quantum phases of matter on a 256-atom programmable quantum simulator. *Nature*, 595(7866):227–232, Jul 2021. ISSN 1476-4687. DOI: [10.1038/s41586-021-03582-4](https://doi.org/10.1038/s41586-021-03582-4). URL <https://doi.org/10.1038/s41586-021-03582-4>.
- [3] Zijun Chen, Kevin J. Satzinger, Juan Atalaya, Alexander N. Korotkov, Andrew Dunsworth, Daniel Sank, Chris Quintana, Matt McEwen, Rami Barends, Paul V. Klimov, Sabrina Hong, Cody Jones, Andre Petukhov, Dvir Kafri, Sean Demura, et al. Exponential suppression of bit or phase errors with cyclic error correction. *Nature*, 595(7867):383–387, Jul 2021. ISSN 1476-4687. DOI: [10.1038/s41586-021-03588-y](https://doi.org/10.1038/s41586-021-03588-y). URL <https://doi.org/10.1038/s41586-021-03588-y>.
- [4] Pascal Scholl, Michael Schuler, Hannah J. Williams, Alexander A. Eberharter, Daniel Barredo, Kai-Niklas Schymik, Vincent Lienhard, Louis-Paul Henry, Thomas C. Lang, Thierry Lahaye, Andreas M. Läuchli, and Antoine Browaeys. Quantum simulation of 2d antiferromagnets with hundreds of rydberg atoms. *Nature*, 595(7866):233–238, jul 2021. DOI: [10.1038/s41586-021-03585-1](https://doi.org/10.1038/s41586-021-03585-1). URL <https://doi.org/10.1038/s41586-021-03585-1>.
- [5] Christopher E Granade, Christopher Ferrie, Nathan Wiebe, and D G Cory. Robust online hamiltonian learning. *New Journal of Physics*, 14(10):103013, oct 2012. DOI: [10.1088/1367-2630/14/10/103013](https://doi.org/10.1088/1367-2630/14/10/103013). URL <https://doi.org/10.1088/1367-2630/14/10/103013>.
- [6] Sheng-Tao Wang, Dong-Ling Deng, and L-M Duan. Hamiltonian tomography for quantum many-body systems with arbitrary couplings. *New Journal of Physics*, 17(9):093017, sep 2015. DOI: [10.1088/1367-2630/17/9/093017](https://doi.org/10.1088/1367-2630/17/9/093017). URL <https://doi.org/10.1088/1367-2630/17/9/093017>.
- [7] Anurag Anshu, Srinivasan Arunachalam, Tomotaka Kuwahara, and Mehdi Soleimanifar. Sample-efficient learning of interacting quantum systems. *Nature Physics*, 17(8):931–935, Aug 2021. ISSN 1745-2481. DOI: [10.1038/s41567-021-01232-0](https://doi.org/10.1038/s41567-021-01232-0). URL <https://doi.org/10.1038/s41567-021-01232-0>.

doi.org/10.1038/s41567-021-01232-0.

- [8] Daniel Burgarth, Koji Maruyama, and Franco Nori. Indirect quantum tomography of quadratic hamiltonians. *New Journal of Physics*, 13(1):013019, Jan 2011. DOI: [10.1088/1367-2630/13/1/013019](https://doi.org/10.1088/1367-2630/13/1/013019). URL <https://doi.org/10.1088/1367-2630/13/1/013019>.
- [9] Ruichao Ma, Clai Owens, Aman LaChapelle, David I. Schuster, and Jonathan Simon. Hamiltonian tomography of photonic lattices. *Phys. Rev. A*, 95:062120, Jun 2017. DOI: [10.1103/PhysRevA.95.062120](https://doi.org/10.1103/PhysRevA.95.062120). URL <https://link.aps.org/doi/10.1103/PhysRevA.95.062120>.
- [10] Jared H. Cole, Sonia G. Schirmer, Andrew D. Greentree, Cameron J. Wellard, Daniel K. L. Oi, and Lloyd C. L. Hollenberg. Identifying an experimental two-state hamiltonian to arbitrary accuracy. *Phys. Rev. A*, 71:062312, Jun 2005. DOI: [10.1103/PhysRevA.71.062312](https://doi.org/10.1103/PhysRevA.71.062312). URL <https://link.aps.org/doi/10.1103/PhysRevA.71.062312>.
- [11] Jared H. Cole, Andrew D. Greentree, Daniel K. L. Oi, Sonia G. Schirmer, Cameron J. Wellard, and Lloyd C. L. Hollenberg. Identifying a two-state hamiltonian in the presence of decoherence. *Physical Review A*, 73(6), Jun 2006. ISSN 1094-1622. DOI: [10.1103/PhysRevA.73.062333](https://doi.org/10.1103/PhysRevA.73.062333). URL <https://doi.org/10.1103/PhysRevA.73.062333>.
- [12] Daniel Burgarth and Kazuya Yuasa. Quantum system identification. *Phys. Rev. Lett.*, 108:080502, Feb 2012. DOI: [10.1103/PhysRevLett.108.080502](https://doi.org/10.1103/PhysRevLett.108.080502). URL <https://link.aps.org/doi/10.1103/PhysRevLett.108.080502>.
- [13] Nathan Wiebe, Christopher Granade, Christopher Ferrie, and D.G. Cory. Hamiltonian learning and certification using quantum resources. *Physical Review Letters*, 112(19), May 2014. ISSN 1079-7114. DOI: [10.1103/PhysRevLett.112.190501](https://doi.org/10.1103/PhysRevLett.112.190501). URL <https://doi.org/10.1103/PhysRevLett.112.190501>.
- [14] Jianwei Wang, Stefano Paesani, Raffaele Santagati, Sebastian Knauer, Antonio A. Gentile, Nathan Wiebe, Maurangelo Petruzzella, Jeremy L. O'Brien, John G. Rarity, Anthony Laing, and et al. Experimental quantum hamiltonian learning. *Nature Physics*, 13(6):551–555, Mar 2017. ISSN 1745-2481. DOI: [10.1038/nphys4074](https://doi.org/10.1038/nphys4074). URL <https://doi.org/10.1038/nphys4074>.
- [15] Eyal Bairey, Itai Arad, and Netanel H. Lindner. Learning a local hamiltonian from local measurements. *Physical Review Letters*, 122(2), Jan 2019. ISSN 1079-7114. DOI: [10.1103/PhysRevLett.122.020504](https://doi.org/10.1103/PhysRevLett.122.020504). URL <https://doi.org/10.1103/PhysRevLett.122.020504>.
- [16] Xiao-Liang Qi and Daniel Ranard. Determining a local Hamiltonian from a single eigenstate. *Quantum*, 3:159, July 2019. ISSN 2521-327X. DOI: [10.22331/q-2019-07-08-159](https://doi.org/10.22331/q-2019-07-08-159). URL <https://doi.org/10.22331/q-2019-07-08-159>.
- [17] Eli Chertkov and Bryan K. Clark. Computational inverse method for constructing spaces of quantum models from wave functions. *Phys. Rev. X*, 8:031029, Jul 2018. DOI: [10.1103/PhysRevX.8.031029](https://doi.org/10.1103/PhysRevX.8.031029). URL <https://link.aps.org/doi/10.1103/PhysRevX.8.031029>.
- [18] Martin Greiter, Vera Schnells, and Ronny Thomale. Method to identify parent hamiltonians for trial states. *Phys. Rev. B*, 98:081113, Aug 2018. DOI: [10.1103/PhysRevB.98.081113](https://doi.org/10.1103/PhysRevB.98.081113). URL <https://link.aps.org/doi/10.1103/PhysRevB.98.081113>.
- [19] Shi-Yao Hou, Ningping Cao, Sirui Lu, Yi Shen, Yiu-Tung Poon, and Bei Zeng. Determining system hamiltonian from eigenstate measurements without correlation functions. *New Journal of Physics*, 22(8):083088, Sep 2020. ISSN 1367-2630. DOI: [10.1088/1367-2630/abaacf](https://doi.org/10.1088/1367-2630/abaacf). URL <https://doi.org/10.1088/1367-2630/abaacf>.
- [20] Chenfeng Cao, Shi-Yao Hou, Ningping Cao, and Bei Zeng. Supervised learning in hamiltonian reconstruction from local measurements on eigenstates. *Journal of Physics: Condensed Matter*, 33(6):064002, Feb 2020. ISSN 1361-648X. DOI: [10.1088/1361-648x/abc4cf](https://doi.org/10.1088/1361-648x/abc4cf). URL <https://doi.org/10.1088/1361-648x/abc4cf>.
- [21] X. Turkeshi, T. Mendes-Santos, G. Giudici, and M. Dalmonte. Entanglement-guided search for parent hamiltonians. *Phys. Rev. Lett.*, 122:150606, Apr 2019. DOI: [10.1103/PhysRevLett.122.150606](https://doi.org/10.1103/PhysRevLett.122.150606). URL <https://doi.org/10.1103/PhysRevLett.122.150606>.

- <https://link.aps.org/doi/10.1103/PhysRevLett.122.150606>.
- [22] Xhek Turkeshi and Marcello Dalmonte. Parent Hamiltonian Reconstruction of Jastrow-Gutzwiller Wavefunctions. *SciPost Phys.*, 8:42, 2020. DOI: [10.21468/SciPostPhys.8.3.042](https://doi.org/10.21468/SciPostPhys.8.3.042). URL <https://scipost.org/10.21468/SciPostPhys.8.3.042>.
- [23] Eugene F. Dumitrescu and Pavel Lougovski. Hamiltonian assignment for open quantum systems. *Phys. Rev. Research*, 2:033251, Aug 2020. DOI: [10.1103/PhysRevResearch.2.033251](https://doi.org/10.1103/PhysRevResearch.2.033251). URL <https://link.aps.org/doi/10.1103/PhysRevResearch.2.033251>.
- [24] Eyal Bairey, Chu Guo, Dario Poletti, Netanel H Lindner, and Itai Arad. Learning the dynamics of open quantum systems from their steady states. *New Journal of Physics*, 22(3):032001, Mar 2020. ISSN 1367-2630. DOI: [10.1088/1367-2630/ab73cd](https://doi.org/10.1088/1367-2630/ab73cd). URL <http://dx.doi.org/10.1088/1367-2630/ab73cd>.
- [25] Assaf Zubida, Elad Yitzhaki, Netanel H. Lindner, and Eyal Bairey. Optimal short-time measurements for hamiltonian learning, 2021. URL <https://arxiv.org/abs/2108.08824>.
- [26] Dominik Hangleiter, Ingo Roth, Jens Eisert, and Pedram Roushan. Precise hamiltonian identification of a superconducting quantum processor, 2021. URL <https://arxiv.org/abs/2108.08319>.
- [27] Arkopal Dutt, Edwin Pednault, Chai Wah Wu, Sarah Sheldon, John Smolin, Lev Bishop, and Isaac L. Chuang. Active learning of quantum system hamiltonians yields query advantage, 2021. URL <https://arxiv.org/abs/2112.14553>.
- [28] Davide Rattacaso, Gianluca Passarelli, Antonio Mezzacapo, Procolo Lucignano, and Rosario Fazio. Optimal parent hamiltonians for time-dependent states. *Physical Review A*, 104(2), Aug 2021. ISSN 2469-9934. DOI: [10.1103/physreva.104.022611](https://doi.org/10.1103/physreva.104.022611). URL <http://dx.doi.org/10.1103/PhysRevA.104.022611>.
- [29] Alexandru Gheorghiu, Theodoros Kapourniotis, and Elham Kashefi. Verification of quantum computation: An overview of existing approaches. *Theory of Computing Systems*, 63(4):715–808, Jul 2018. ISSN 1433-0490. DOI: [10.1007/s00224-018-9872-3](https://doi.org/10.1007/s00224-018-9872-3). URL <http://dx.doi.org/10.1007/s00224-018-9872-3>.
- [30] Jens Eisert, Dominik Hangleiter, Nathan Walk, Ingo Roth, Damian Markham, Rhea Parekh, Ulysse Chabaud, and Elham Kashefi. Quantum certification and benchmarking. *Nature Reviews Physics*, 2(7):382–390, Jun 2020. ISSN 2522-5820. DOI: [10.1038/s42254-020-0186-4](https://doi.org/10.1038/s42254-020-0186-4). URL <http://dx.doi.org/10.1038/s42254-020-0186-4>.
- [31] Ivan Šupić and Joseph Bowles. Self-testing of quantum systems: a review. *Quantum*, 4:337, September 2020. ISSN 2521-327X. DOI: [10.22331/q-2020-09-30-337](https://doi.org/10.22331/q-2020-09-30-337). URL <https://doi.org/10.22331/q-2020-09-30-337>.
- [32] Jose Carrasco, Andreas Elben, Christian Kokail, Barbara Kraus, and Peter Zoller. Theoretical and experimental perspectives of quantum verification. *PRX Quantum*, 2:010102, Mar 2021. DOI: [10.1103/PRXQuantum.2.010102](https://doi.org/10.1103/PRXQuantum.2.010102). URL <https://link.aps.org/doi/10.1103/PRXQuantum.2.010102>.
- [33] Martin Kliesch and Ingo Roth. Theory of quantum system certification. *PRX Quantum*, 2:010201, Jan 2021. DOI: [10.1103/PRXQuantum.2.010201](https://doi.org/10.1103/PRXQuantum.2.010201). URL <https://link.aps.org/doi/10.1103/PRXQuantum.2.010201>.
- [34] Agnes Valenti, Evert van Nieuwenburg, Sebastian Huber, and Eliska Greplova. Hamiltonian learning for quantum error correction. *Physical Review Research*, 1(3), Nov 2019. ISSN 2643-1564. DOI: [10.1103/physrevresearch.1.033092](https://doi.org/10.1103/physrevresearch.1.033092). URL <http://dx.doi.org/10.1103/PhysRevResearch.1.033092>.
- [35] Marcus P. da Silva, Olivier Landon-Cardinal, and David Poulin. Practical characterization of quantum devices without tomography. *Phys. Rev. Lett.*, 107:210404, Nov 2011. DOI: [10.1103/PhysRevLett.107.210404](https://doi.org/10.1103/PhysRevLett.107.210404). URL <https://link.aps.org/doi/10.1103/PhysRevLett.107.210404>.
- [36] Christian Gogolin and Jens Eisert. Equilibration, thermalisation, and the emergence of statistical mechanics in closed quantum systems. *Reports on Progress in Physics*, 79(5):056001, Apr 2016. ISSN 1361-6633. DOI: [10.1088/0034-4885/79/5/056001](https://doi.org/10.1088/0034-4885/79/5/056001). URL <https://doi.org/10.1088/0034-4885/79/5/056001>.

<http://dx.doi.org/10.1088/0034-4885/79/5/056001>.

- [37] Clemens Neuenhahn and Florian Marquardt. Thermalization of interacting fermions and delocalization in fock space. *Physical Review E*, 85(6), Jun 2012. ISSN 1550-2376. DOI: [10.1103/PhysRevE.85.060101](https://doi.org/10.1103/PhysRevE.85.060101). URL <http://dx.doi.org/10.1103/PhysRevE.85.060101>.
- [38] Elena Canovi, Davide Rossini, Rosario Fazio, Giuseppe E. Santoro, and Alessandro Silva. Quantum quenches, thermalization, and many-body localization. *Phys. Rev. B*, 83:094431, Mar 2011. DOI: [10.1103/PhysRevB.83.094431](https://doi.org/10.1103/PhysRevB.83.094431). URL <https://link.aps.org/doi/10.1103/PhysRevB.83.094431>.
- [39] Anatoli Polkovnikov, Krishnendu Sengupta, Alessandro Silva, and Mukund Vengalattore. Colloquium: Nonequilibrium dynamics of closed interacting quantum systems. *Reviews of Modern Physics*, 83(3):863–883, Aug 2011. ISSN 1539-0756. DOI: [10.1103/revmodphys.83.863](https://doi.org/10.1103/revmodphys.83.863). URL <http://dx.doi.org/10.1103/RevModPhys.83.863>.
- [40] Easwar Magesan and Jay M. Gambetta. Effective hamiltonian models of the cross-resonance gate. *Phys. Rev. A*, 101:052308, May 2020. DOI: [10.1103/PhysRevA.101.052308](https://doi.org/10.1103/PhysRevA.101.052308). URL <https://link.aps.org/doi/10.1103/PhysRevA.101.052308>.
- [41] Thomas M. Cover and Joy A. Thomas. *Elements of Information Theory 2nd Edition (Wiley Series in Telecommunications and Signal Processing)*. Wiley-Interscience, July 2006. ISBN 0471241954.
- [42] MD SAJID ANIS, Héctor Abraham, AduOf-
fei, Rochisha Agarwal, Gabriele Agliardi,
Merav Aharoni, Ismail Yunus Akhalwaya,
Gadi Aleksandrowicz, Thomas Alexander,
Matthew Amy, Sashwat Anagolum, Eli Ar-
bel, Abraham Asfaw, Anish Athalye, Artur
Avkhadiev, et al. Qiskit: An open-source
framework for quantum computing, 2021.
- [43] Chad Rigetti and Michel Devoret. Fully
microwave-tunable universal gates in super-
conducting qubits with linear couplings and
fixed transition frequencies. *Phys. Rev. B*,
81:134507, Apr 2010. DOI: [10.1103/PhysRevB.81.134507](https://doi.org/10.1103/PhysRevB.81.134507). URL <https://link.aps.org/doi/10.1103/PhysRevB.81.134507>.
- [44] Jerry M. Chow, A. D. Córcoles, Jay M.
Gambetta, Chad Rigetti, B. R. John-
son, John A. Smolin, J. R. Rozen,
George A. Keefe, Mary B. Rothwell,
Mark B. Ketchen, and M. Steffen. Simple
all-microwave entangling gate for fixed-
frequency superconducting qubits. *Phys.
Rev. Lett.*, 107:080502, Aug 2011. DOI:
[10.1103/PhysRevLett.107.080502](https://doi.org/10.1103/PhysRevLett.107.080502). URL
[https://link.aps.org/doi/10.1103/
PhysRevLett.107.080502](https://link.aps.org/doi/10.1103/PhysRevLett.107.080502).
- [45] Sarah Sheldon, Easwar Magesan, Jerry M.
Chow, and Jay M. Gambetta. Procedure
for systematically tuning up cross-talk in
the cross-resonance gate. *Phys. Rev. A*,
93:060302, Jun 2016. DOI: [10.1103/PhysRevA.93.060302](https://doi.org/10.1103/PhysRevA.93.060302). URL <https://link.aps.org/doi/10.1103/PhysRevA.93.060302>.
- [46] Hamiltonian tomography.
URL [https://qiskit.org/
textbook/ch-quantum-hardware/
hamiltonian-tomography.html](https://qiskit.org/textbook/ch-quantum-hardware/hamiltonian-tomography.html). Accessed:
2022-03-29.
- [47] Paolo Zanardi, Paolo Giorda, and Marco
Cozzini. Information-theoretic differential
geometry of quantum phase transitions.
Phys. Rev. Lett., 99:100603, Sep 2007. DOI:
[10.1103/PhysRevLett.99.100603](https://doi.org/10.1103/PhysRevLett.99.100603). URL
[https://link.aps.org/doi/10.1103/
PhysRevLett.99.100603](https://link.aps.org/doi/10.1103/PhysRevLett.99.100603).
- [48] Lorenzo Campos Venuti and Paolo Zanardi.
Quantum critical scaling of the geometric
tensors. *Phys. Rev. Lett.*, 99:095701, Aug
2007. DOI: [10.1103/PhysRevLett.99.095701](https://doi.org/10.1103/PhysRevLett.99.095701). URL
[https://link.aps.org/doi/10.
1103/PhysRevLett.99.095701](https://link.aps.org/doi/10.1103/PhysRevLett.99.095701).
- [49] Damian F. Abasto, Alioscia Hamma, and
Paolo Zanardi. Fidelity analysis of topolog-
ical quantum phase transitions. *Phys. Rev.
A*, 78:010301, Jul 2008. DOI: [10.1103/PhysRevA.78.010301](https://doi.org/10.1103/PhysRevA.78.010301). URL <https://link.aps.org/doi/10.1103/PhysRevA.78.010301>.
- [50] Paolo Zanardi, Lorenzo Campos Venuti,
and Paolo Giorda. Bures metric over
thermal state manifolds and quantum criti-
cality. *Phys. Rev. A*, 76:062318, Dec 2007.
DOI: [10.1103/PhysRevA.76.062318](https://doi.org/10.1103/PhysRevA.76.062318). URL
[https://link.aps.org/doi/10.1103/
PhysRevA.76.062318](https://link.aps.org/doi/10.1103/PhysRevA.76.062318).
- [51] Davide Rattacaso, Patrizia Vitale, and Alioscia Hamma. Quantum geometric tensor away from equilibrium. *Journal of Physics*

A Details of uncertainty estimation

In this appendix, we illustrate the details of the derivation of the bound in Eq. (6).

The uncertainty on B_i is

$$\delta B_i = \sqrt{\sum_{\gamma,m} \left(\frac{\partial B_i}{\partial r_\gamma(t_m)} \sigma(r_\gamma(t_m)) \right)^2} + \sum_m |\text{Tr}(-i[L_i, \rho(t_m)] R_m)| \quad (16)$$

We want to find an upper bound on this uncertainty that does not depend on the states $\{\rho(t_m)\}$.

The first term in the previous equation contains the statistical uncertainty. In a spin system we can choose basis operators as normalized tensor products of Pauli operators, hence $O_\alpha^2 = \mathbf{1}/2^{N_q}$ and $\sigma(r_\alpha(t_n)) = 1/\sqrt{2^{N_q} N_M}$. It follows that

$$\delta B_i = \frac{1}{\sqrt{2^{N_q} N_M}} \sqrt{\sum_{\gamma,m} \left(\frac{\partial B_i}{\partial r_\gamma(t_m)} \right)^2} + \sum_m |\text{Tr}(-i[L_i, \rho(t_m)] R_m)| \quad (17)$$

Since

$$B_i = \sum_{n\alpha\beta} \text{Tr}(-i[L_i, O_\alpha] O_\beta) r_\alpha(t_n) (r_\beta(t_{n+1}) - r_\beta(t_n)) / \delta t, \quad (18)$$

we can take the derivative to obtain

$$\begin{aligned} \sum_{\gamma,m} \left(\frac{\partial B_i}{\partial r_\gamma(t_m)} \right)^2 &= \sum_{\gamma,m} \left(\sum_{n,\alpha\beta} \text{Tr}(-i[L_i, O_\alpha] O_\beta) \left[\delta_{\alpha\gamma} \delta_{nm} \frac{r_\beta(t_{n+1}) - r_\beta(t_n)}{\delta t} + r_{\beta n} \delta_{\gamma\alpha} \frac{\delta_{mn} - \delta_{m,n+1}}{\delta t} \right] \right)^2 \\ &= \sum_{\gamma,m} \left(\sum_{\beta} \text{Tr}(-i[L_i, O_\gamma] O_\beta) \left[\frac{r_\beta(t_{m+1}) - r_\beta(t_m)}{\delta t} + \frac{r_\beta(t_m) - r_\beta(t_{m-1})}{\delta t} \right] \right)^2 + o(N_T) \\ &\approx \sum_{\gamma,m} \left(\sum_{\beta} \text{Tr}(-i[L_i, O_\beta] O_\gamma) \left[\frac{r_\beta(t_{m+1}) - r_\beta(t_{m-1})}{\delta t} \right] \right)^2. \end{aligned} \quad (19)$$

At this point we approximate the fraction with the derivative and exploit the fact that $\{O_\alpha\}$ is an orthonormal basis:

$$\begin{aligned} \sum_{\gamma,m} \left(\frac{\partial B_i}{\partial r_\gamma(t_m)} \right)^2 &\approx 4 \sum_{\gamma,m} \left(\sum_{\beta} \text{Tr}(-i[L_i, O_\beta] O_\gamma) \partial_t r_\beta(t_m) \right)^2 \\ &= 4 \sum_{\gamma,m} (\text{Tr}(-i[L_i, \partial_t \rho(t_m)] O_\gamma))^2 \\ &= 4 \sum_{\gamma,m} (\text{Tr}(-i[L_i, \partial_t \rho(t_m)]))^2. \end{aligned} \quad (20)$$

Replacing this estimate of the statistical uncertainty and the Taylor remainder $R_n = \frac{-[H_i, [H, \rho(t_n^*)]]}{2}$ in the total uncertainty δB_i , we obtain

$$\delta B_i \approx \frac{2}{\sqrt{2^{N_q} N_M}} \sqrt{\sum_m (\text{Tr}(-i[L_i, \partial_t \rho(t_m)]))^2} + \frac{\delta t}{2} \sum_m |\text{Tr}((-i[L_i, \rho(t_m)]) (-[H, [H, \rho(t_m^*)]]))|, \quad (21)$$

where H is the system Hamiltonian.

Considering the Cauchy-Schwarz inequality $|\text{Tr}(AB)| \leq \sqrt{\text{Tr}(AA)\text{Tr}(BB)}$, this last estimate can be bounded as

$$\delta B_i \leq \frac{2}{\sqrt{2^{N_q} N_M}} \sqrt{\sum_m \left(\text{Tr}(-i[L_i, -i[H, \rho(t_m)]]) \right)^2} + \frac{\delta t}{2} \sum_m \sqrt{\text{Tr} \left((i[L_i, \rho(t_m)])^2 \right) \text{Tr}([H, [H, \rho(t_m^*)])^2}, \quad (22)$$

where we have taken into account that $\partial_t \rho(t_m) = -i[H, \rho(t_m)]$.

Now we need to understand how the commutator with an Hermitian operators changes the Frobenius norm of a given operator. In particular, given a Hermitian operator A with spectral decomposition $A = \sum_i a_i |i\rangle\langle i|$, we define $a_{\min} = \min(a_i)$, $a_{\max} = \max(a_i)$, and $A_\delta = A - a_{\min} \mathbf{1}$. Hence we can write

$$\begin{aligned} \text{Tr}[(-i[A, X])^2] &= \text{Tr}[(-i[A_\delta, X])^2] \\ &= 2[\text{Tr}(XXA_\delta A_\delta) - \text{Tr}(A_\delta X A_\delta X)] \\ &= 2 \sum_{ij} (a_i - a_{\min})(a_i - a_j) |\langle i|X|j\rangle|^2 \\ &\leq 2(a_{\max} - a_{\min})^2 \sum_{ij} |\langle i|X|j\rangle|^2 \\ &= 2\|A_\delta\|_{\text{op}}^2 \text{Tr}(X^2), \end{aligned} \quad (23)$$

where $\|A_\delta\|_{\text{op}}$ is the operator norm of A_δ .

Replacing this bound in our estimate of the uncertainty δB_i and considering that the purity of the state $\rho(t)$ is $\text{Tr}(\rho(t)^2) \leq 1$ for each value of t , we obtain

$$\begin{aligned} \delta B_i &\leq \frac{2\|L_i\|_{\text{op}}}{\sqrt{2^{N_q} N_T}} \sqrt{\sum_m 2 \left(\text{Tr}(-i[H, \rho(t_m)]) \right)^2} + \|L_{i,\delta}\|_{\text{op}} \|H_\delta\|_{\text{op}} \sum_m \sqrt{\text{Tr} \left((-i[H, \rho(t_m^*)])^2 \right)} \\ &\leq \frac{4\|H_\delta\|_{\text{op}} \|L_{i,\delta}\|_{\text{op}}}{\sqrt{2^{N_q} N_M}} \sqrt{N_T} + \delta t \|L_{i,\delta}\|_{\text{op}} \|H_\delta\|_{\text{op}}^2 N_T, \end{aligned} \quad (24)$$

where $\|L_{i,\delta}\|_{\text{op}}$ and $\|H_\delta\|_{\text{op}}$ are the difference between the maximum and the minimum eigenvalues of H and L_i , respectively.

For a traceless operator $A = \sum_i a_i |i\rangle\langle i|$ we have that the maximum eigenvalue is positive and the minimum one is negative, therefore

$$\|A_\delta\|_{\text{op}} = a_{\max} - a_{\min} = |a_{\max}| + |a_{\min}| \leq 2\max(|a_i|) = 2\|A\|_{\text{op}}. \quad (25)$$

Hence, since both H and L_i are traceless and since we can choose without loss of generality $\|L_i\|_{\text{op}} = \|L\|_{\text{op}} \forall i$, the last inequality becomes

$$\delta B_i \leq \frac{16\|H\|_{\text{op}} \|L\|_{\text{op}}}{\sqrt{2^{N_q} N_M}} \sqrt{N_T} + 4\delta t \|L\|_{\text{op}} \|H\|_{\text{op}}^2 N_T. \quad (26)$$

An analogous bound on the uncertainty about the Hamiltonian couplings can be calculated propagating the uncertainty about B_i . When $\|V^{-1}\| \ll 1$ we obtain

$$\delta h_i = \sum_j (V^{-1})_{ij} \delta B_j. \quad (27)$$

and therefore

$$\|\vec{\delta h}\| \leq \sqrt{\text{Tr}(V^{-2})} \|L\|_{\text{op}} \left(16\|H\|_{\text{op}} \sqrt{\frac{N_T}{2^{N_q} N_M}} + 4N_T \|H\|_{\text{op}}^2 \delta t \right). \quad (28)$$

When $\|V^{-1}\| \ll 1$ does not hold, this estimate for the uncertainty fails, but this is the case in which we have an uncertainty that is so large that finding the exact Hamiltonian is impossible.

Now, we want to derive a bound on the relative uncertainty on the couplings. Taking into account the triangular inequality and the relationship between p -norms, and defining l as the number of Hamiltonian couplings, we can write

$$\|H\|_{\text{op}} = \left\| \sum_i h_i L_i \right\|_{\text{op}} \leq \sum_i |h_i| \|L_i\|_{\text{op}} = \|L\|_{\text{op}} \sum_i |h_i| \leq \sqrt{l} \|L\|_{\text{op}} \|\vec{h}\|, \quad (29)$$

from which we finally obtain

$$\frac{\|\vec{\delta h}\|}{\|\vec{h}\|} \leq \sqrt{l \text{Tr}(V^{-2})} \|L\|_{\text{op}}^2 \left(16 \sqrt{\frac{N_T}{2^{N_a} N_M}} + 4N_T \|H\|_{\text{op}} \delta t \right). \quad (30)$$